nature communications

Article

https://doi.org/10.1038/s41467-024-52387-2

Substantial increase of organic carbon storage in Chinese lakes

Received: 28 June 2024

Accepted: 3 September 2024

Published online: 14 September 2024

Check for updates

Dong Liu[1,2], Kun Shi[1,3] ✉, Peng Chen[4], Nuoxiao Yan[1], Lishan Ran[5], Tiit Kutser[6], Andrew N. Tyler[2], Evangelos Spyrakos[2], R. Iestyn Woolway[7], Yunlin Zhang[1,3] & Hongtao Duan[1] ✉

Previous studies typically assumed a constant total organic carbon (OC) storage in the lake water column, neglecting its significant variability within a changing world. Based on extensive field data and satellite monitoring techniques, we demonstrate considerable spatiotemporal variability in OC concentration and storage for 24,366 Chinese lakes during 1984–2023. Here we show that dissolved OC concentration is high in northwest saline lakes and particulate OC concentration is high in southeast eutrophic lakes. Along with increasing OC concentration and water volume, dissolved and particulate OC storage increase by 44.6% and 33.5%, respectively. Intensified human activities, water input, and wind disturbance are the key drivers for increasing OC storage. Moreover, higher OC storage further leads to an 11.0% increase in nationwide OC burial and a decrease in carbon emissions from 71.1% of northwest lakes. Similar changes are occurring globally, which suggests that lakes are playing an increasingly important role in carbon sequestration.

Lakes serve as recipients, regulators, reactors, and storages in the global carbon cycle[1,2]. Globally, inland waters receive 2.9–5.1 Tg C yr^{-1} from terrestrial ecosystems[1,3]; lakes and reservoirs bury 0.06–0.25 Mt C yr^{-1} into the sediment[4]; and lakes and reservoirs emit 0.06–0.84 Tg C yr^{-1} of CO_2 to the atmosphere[5], and export 0.8–1.1 Tg C yr^{-1} to the oceans[2]. The remaining carbon is partly preserved in lake waters by either organic or inorganic forms[6,7]. Total organic carbon (OC) storage is defined as the product of lake OC concentration and water volume[8]. Lake OC storage affects several processes, including phytoplankton photosynthesis by absorbing sunlight[6,9], dissolved oxygen consumption[10,11], and lake carbon burial and outgassing[4,5]. Despite its importance, research on large-scale changes in lake OC storage is limited. Previous studies primarily focused on OC production and mineralization[12,13], spatiotemporal changes in OC concentration and composition[14,15], and/or carbon balance estimation by assuming a constant OC storage[1–3]. However, the amount of OC stored in lakes varies due to, for example, phytoplankton growth, water volume, and sewage discharge[8,16,17].

In recent decades, lakes around the world have changed under the pressures of climate warming and intensifying human activities[18]. Algal blooms in many lakes are now occurring more frequently, with 8.8% of lakes worldwide experiencing an increase in bloom risk between the 1980s and 2010s[19,20]. Water volumes in 79.4% of global lakes has also increased since 2003, and one of the five hotspots of such change is China's Tibetan Plateau[21–23]. Along with the changes in algal biomass, satellite-based monitoring of eutrophic Lake Taihu, China, has suggested that both dissolved (DOC) and particulate OC (POC) concentrations have fluctuated significantly in recent decades[17,24]. Lake OC storage is expected to vary greatly, as the changes in OC concentration and/or water volume. However, there is little research on the spatiotemporal variations of OC storage in various lakes. A study focusing on

[1]Key Laboratory of Lake and Watershed Science for Water Security, Nanjing Institute of Geography and Limnology, Chinese Academy of Sciences, Nanjing, China. [2]Biological and Environmental Sciences, School of Natural Sciences, University of Stirling, Stirling, UK. [3]Ecosystem Research Station of Lake Qiandaohu, Nanjing Institute of Geography and Limnology, Chinese Academy of Sciences, Nanjing, China. [4]State Key Laboratory of Satellite Ocean Environment Dynamics, Second Institute of Oceanography, Ministry of Natural Resources, Hangzhou, China. [5]Department of Geography, The University of Hong Kong, Hong Kong, Hong Kong. [6]Estonian Marine Institute, University of Tartu, Tallinn, Estonia. [7]School of Ocean Sciences, Bangor University, Menai Bridge, Anglesey, UK. ✉e-mail: kshi@niglas.ac.cn; htduan@niglas.ac.cn

changes in OC storage across a wider range of lakes can provide valuable insights into the global carbon cycle.

China encompasses 24,366 lakes that are larger than 0.01 km^2, and distributed across five limnetic zones characterized by diverse topographies and climatic conditions[25,26]: the Inner Mongolia-Xinjiang Lake zone (IMXL), the Tibetan Plateau Lake zone (TPL), the Yunnan-Guizhou Plateau Lake zone (YGPL), the Northeast Plain and Mountain Lake zone (NPML), and the Eastern Plain Lake zone (EPL). Across China, climatic conditions and human activities are clearly different on both sides of the Hu-line (Supplementary Fig. 3). Compared to the northwest IXML and TPL zones of the Hu-line, the three southeast lake zones had higher precipitation and more human activities[25]. Moreover, in recent decades, climatic warming has led to the expansion of lakes in the TPL[23], and intensifying human activities have caused universal lake eutrophication in the EPL[25]. Therefore, China is an ideal region to explore the spatiotemporal changes in lake OC storage in a changing world.

In this work, based on extensive field data and satellite monitoring techniques, we derive DOC and POC concentrations from Landsat satellite data, calculate DOC and POC storage by multiplying water volumes, and reveal significant changes in OC concentrations and substantial increases in OC storage across China's 24,366 lakes during 1984–2023 (see "Methods").

Results and discussion

Spatiotemporal differences in OC concentration

Across the studied lakes with an area > 0.01 km^2 from the HydroLAKES dataset i.e., that could be observed using Landsat satellite data (N = 24,366), DOC concentrations followed a spatial pattern of high in the northwest and low in the southeast and showed general increasing trends in different lakes during 1984–2023. Across China, mean DOC in the northwest IMXL and TPL zones (25.71 ± 24.72 mg L^{-1}) was 2.5 times that in the southeast YGPL and EPL zones (10.29 ± 7.27 mg L^{-1}) (Fig. 1a). DOC accumulated along with salinity in the northwest arid/semi-arid lakes. Conversely, strong precipitation diluted DOC concentrations in lakes of southeast China. For the in-situ data, there was a significant positive relationship between the logarithmic DOC concentration and conductivity, with Pearson's r = 0.56 (N = 1636, p < 0.01, Supplementary Fig. 6a). Moreover, algal proliferation also contributed to high DOC concentrations in freshwater lakes (<2000 μs cm^{-1}), as suggested by a positive correlation between the logarithmic in-situ DOC and chlorophyll-a (Chl-a) concentrations (r = 0.23, N = 3624, p < 0.0001). Along with intensifying human activities (Supplementary Fig. 7h), 11,055 of the 15,303 freshwater lakes (i.e., 72.2%) in the southeast NPML and EPL zones showed increased DOC concentrations during 1984–2023 (Fig. 1b). However, 48.7% of lakes in the northwest TPL zone showed decreased DOC concentrations, which may be due to increasing precipitation (Supplementary Fig. 7f). Overall, mean DOC concentration in China's lakes increased from 14.79 ± 12.49 mg L^{-1} in 1984 to 18.14 ± 21.75 mg L^{-1} in 2023, with an increasing trend in 65.4% of lake area.

In contrast to DOC, POC concentrations had a spatial pattern of low in the northwest and high in the southeast and demonstrated clear increasing trends in different lakes during 1984–2023 across China. Mean POC concentration was only 0.83 ± 0.19 mg L^{-1} in the northwest TPL zone, but as high as 4.85 ± 0.65 mg L^{-1} and 2.87 ± 1.08 mg L^{-1} in the southeast NPML and EPL zones, respectively (Fig. 1c). For the IMXL and YGPL zones across the Hu-line, lake POC concentration was also high in the southeast regions. High POC concentration was mainly due to algal proliferation. Total suspended matter (TSM) including algae accounted for only 14.1% of the spatial variations in POC concentration, indicated by the linear relationship between the logarithmic in-situ TSM

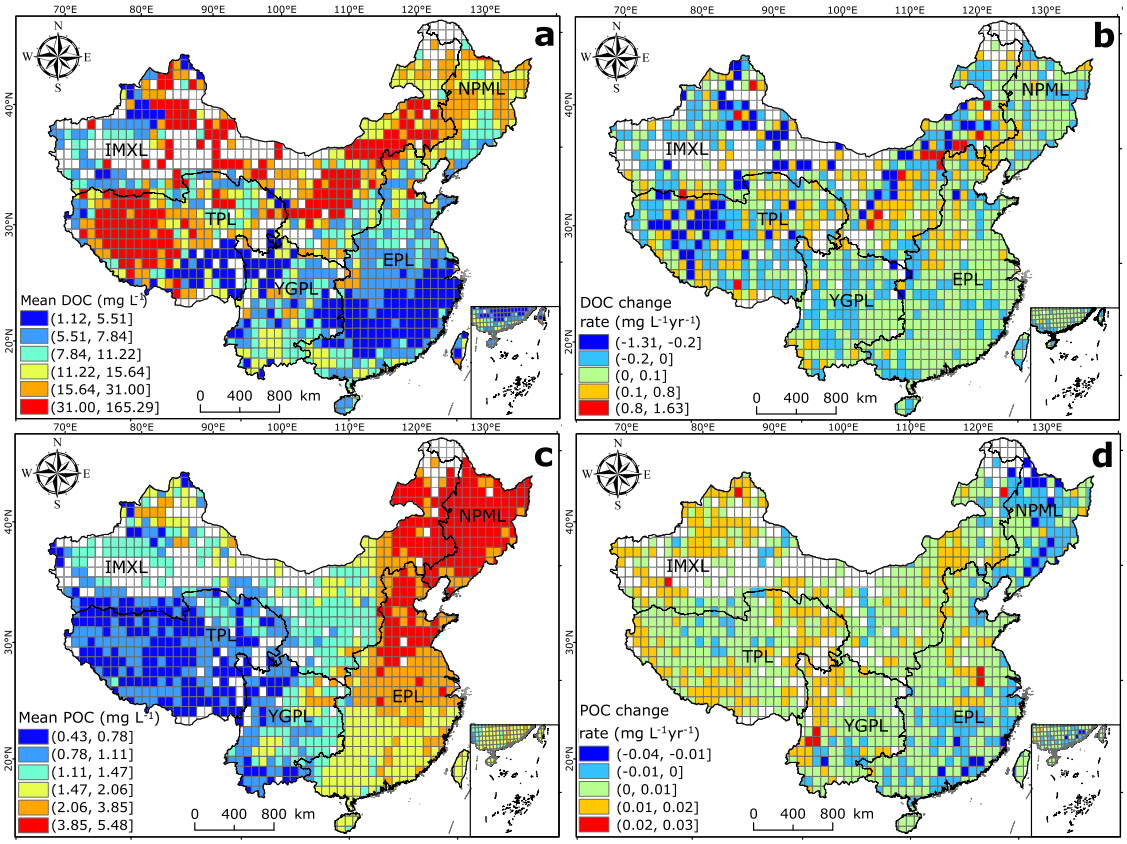

Fig. 1 | Spatiotemporal variations in OC concentrations. Spatial patterns of 1.0° grid-based (**a**) climatologically mean DOC concentration, (**b**) annual DOC change rate, (**c**) climatologically mean POC concentration, and (**d**) annual POC change rate. The satellite-derived annual mean DOC and POC concentrations of 24,366 lakes during 1984–2023 were used to calculate these 1.0° grid-based results. Source data are provided as a Source Data file.

https://doi.org/10.1038/s41467-024-52387-2

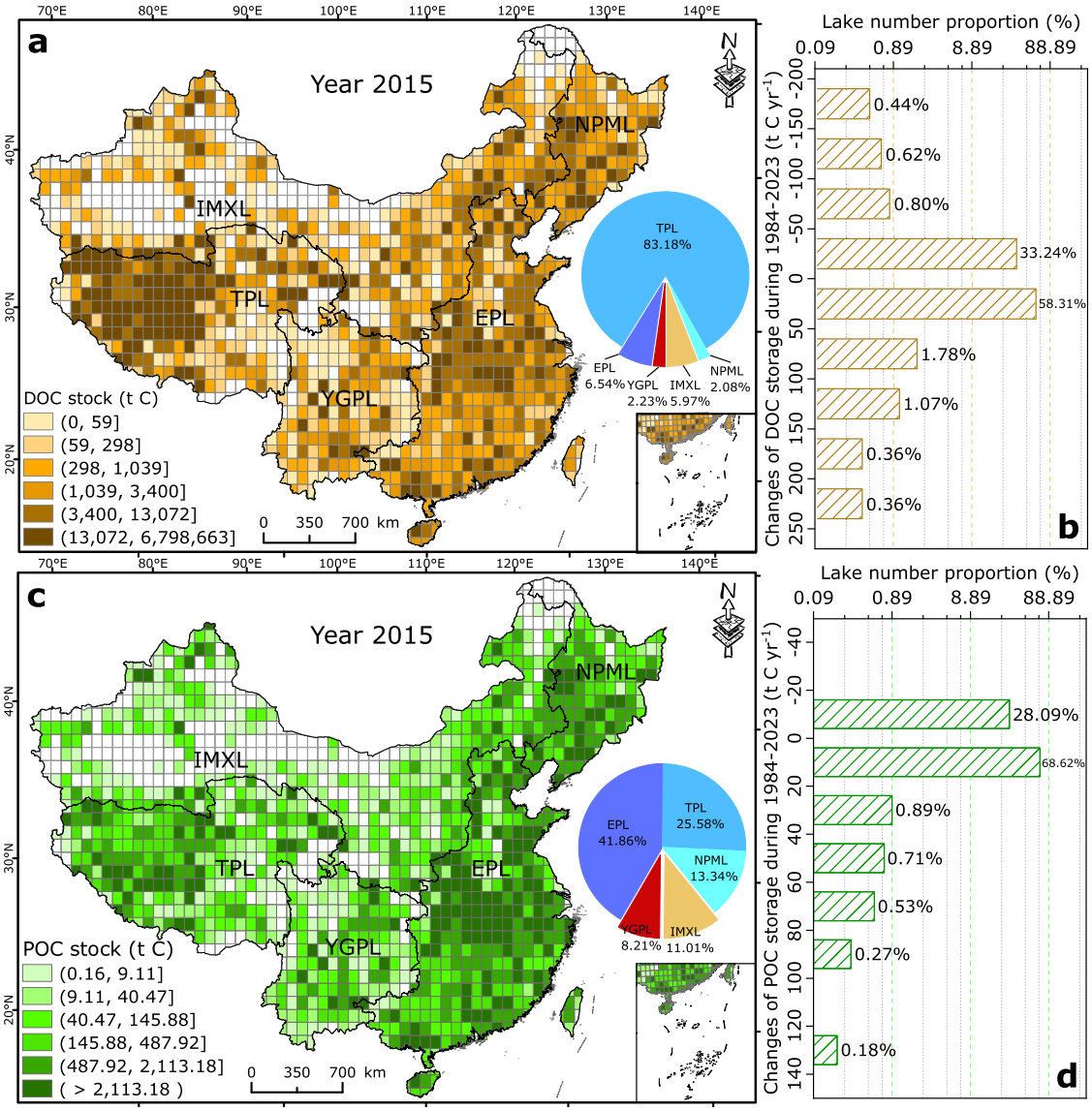

Fig. 2 | Spatiotemporal variations in OC storage. a 1.0° grid-based DOC stock for 24,366 lakes in 2015; (**b**) lake-based changes for 1125 lakes during 1984–2023; (**c**) 1.0° grid-based POC stock for 24,366 lakes in 2015; and (**d**) lake-based changes for 1125 lakes during 1984–2023. The changes of DOC storage mean the linearly fitted slope between DOC storage and year during 1984–2023. Source data are provided as a Source Data file.

and POC concentrations ($N = 2026$, $R^2 = 0.14$, $p < 0.0001$). However, Chl-a alone could explain 71.0% ($N = 2088$, Supplementary Fig. 6b). Therefore, as population density generally grew in China (Supplementary Fig. 7h), 16,007 lakes whose area in total accounted for 80.6% showed increasing POC concentrations during 1984–2023 (Fig. 1d). For the northwest IMXL and TPL zones with low POC concentrations, 93.2% of lake area showed increasing trends. However, for the southeast NPML and EPL zones with high POC concentrations, 59.3% of lake area followed a downward trend, which we anticipate is due to water pollution control since 2000[27]. Namely, human activities have been reducing the spatial differences in POC concentration.

Substantial increase in OC storage

Lake DOC was mainly stored in the TPL zone, and the increase in lake DOC storage during 1984–2023 also mainly occurred in the TPL zone. Combining the derived DOC concentration and water volume data from the HydroLAKES dataset in 2015 (Supplementary Table 1), we estimated that Chinese lakes collectively contained 39.43 Tg C of DOC. 83.2% of this total was stored in the TPL zone, the western endorheic regions of which were particularly notable for their high DOC concentrations (Figs. 1a, 2a). Lakes with low DOC concentrations in the EPL zone stored only 6.5% of DOC but 24.6% of water. Overall, lake-based DOC stock in China was dependent on water storage. The logarithmic DOC stock was linearly correlated with the logarithmic water volume, with $R^2 = 0.81$ and $p < 0.01$ (Supplementary Fig. 6c). Due to increasing DOC concentrations (Fig. 1b) and water volume[23], there was a substantial increase in lake DOC storage during 1984–2023. Of the 1125 lakes with time-series data of water volume, 63.7% experienced an increase in DOC storage (Fig. 2b, Supplementary Fig. 8); moreover, 92.0% of this total increase occurred in the TPL zone with a considerable increase in water volume[23]. According to the average growth rate of 96,295 t C yr^{-1} for the 1125 lakes, we estimated that ~13.05 Tg C of DOC was newly reserved in the 24,366 Chinese lakes during 1984–2023, an increase of 44.6%. In turn, we suggest that Chinese lakes acted as carbon sinks through storing more DOC.

In contrast to DOC storage, lake POC was concentrated in large quantities in lakes of the southeast with high POC concentrations. In 2015, the total POC storage was 2.14 Tg C, with 55.2% in the southeast EPL and NPML zones which stored only 29.3% of water (Fig. 2c). However, whilst lakes in the TPL zone stored 55.3% of water, their POC

https://doi.org/10.1038/s41467-024-52387-2

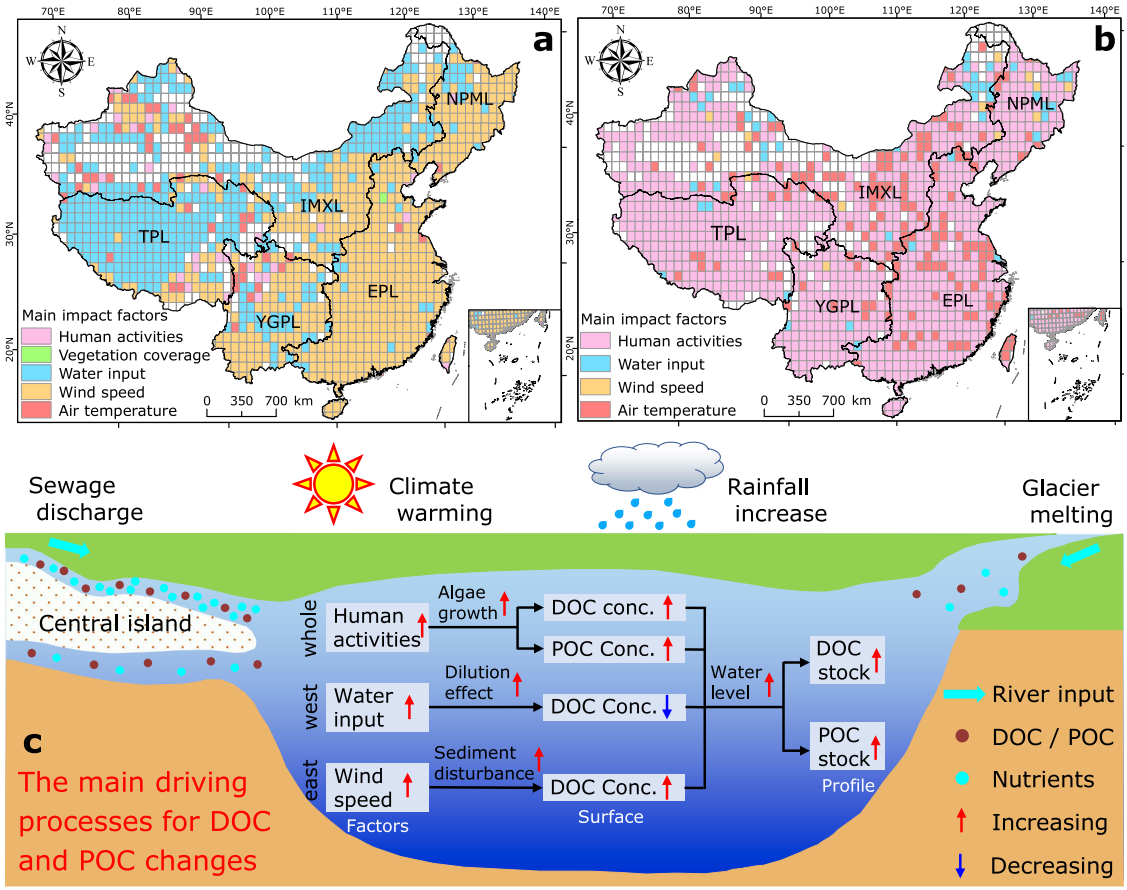

Fig. 3 | Influences of different factors on DOC and POC variations. The main driving factors for the annual changes of (**a**) DOC and (**b**) POC concentrations during 1984–2023. The main driving factors indicate those which have the largest contributions. The figures show the main factors with the largest mean contributions for lakes in the 1.0° grids. **c** The driving processes of the main factors for the changes in DOC and POC. DOC Conc. DOC concentration. POC Conc. POC concentration. Source data are provided as a Source Data file.

reserve was only 25.6%. Lake-based POC storage was generally determined by water volume, as suggested by the positive correlation between the logarithmic POC storage and water volume ($R^2 = 0.87$, Supplementary Fig. 6d). Therefore, similar to DOC, POC storage in Chinese lakes was also elevated due to increasing water volume during 1984–2023. Of the 1125 lakes with time-series of water volume, 71.7% experienced increasing trends of POC storage (Supplementary Fig. 9); as many as 94.3% and 88.9% of lakes in the TPL and YGPL zones followed an upward trend during 1984–2023. Moreover, although 28.1% of lakes had decreasing POC storage, the decline trends were comparatively weak (Fig. 2d). Based on the average growth rate of 4033 t C yr^{-1} for the 1125 lakes, we estimated a total increase of 33.5% in POC storage for all 24,366 Chinese lakes during 1984–2023. Therefore, Chinese lakes also acted as carbon sinks by reserving more POC.

Drivers of change in Lake OC

Lake OC concentration is influenced by both anthropogenic and natural factors[1,3]. By applying the Random Forest analyses, we quantified the relative contributions of different factors to the spatiotemporal variations in OC concentration (Supplementary Note 4). Our results suggested that human activities contributed 50.2% to the spatial changes in DOC concentration and climate factors contributed 75.9% to the spatial changes in POC concentration. Furthermore, human activities, water input, and wind speed commonly had the largest contributions and were identified as the main drivers of the annual changes in OC concentration during 1984–2023 (Fig. 3).

Intensifying human activities elevated lake POC concentrations. Across China, 70.7% of lakes had an increasing population density within their basins during 1984–2023 (Supplementary Fig. 7h); population density was identified as the main factor for POC changes in 72.3% of lakes and had an average contribution of 33.1% (Fig. 3b). Human-induced eutrophication would increase lake phytoplankton, which itself is an important source of autochthonous POC (Supplementary Fig. 6b). For eutrophic lakes in the EPL zone, algal proliferation determines the quantity and composition of POC, and linear relationships between POC and Chl-a are commonly reported[16,28]. Moreover, Hou et al.[19] reported that 88.9% of freshwater lakes in China showed increasing algal bloom frequencies during the 1980s–2010s. Meanwhile, half of the saline lakes in the remote TPL zone also experienced Chl-a increases due to increased riverine nutrient input[29].

We suggest that increasing water input diluted lake DOC concentrations in the northwest IMXL and TPL zones. For the 7716 lakes situated in these two zones, increased precipitation and/or decreased evaporation occurred in 95.4% of them (Supplementary Fig. 7); and water input-related factors (precipitation, runoff, and evaporation) had a mean contribution of 37.3% for DOC concentration changes during 1984–2023 (Fig. 3a). Due to increasing water input associated with glacial ablation and/or climatic humidification, area expansion and salinity reduction are widespread for lakes in the IMXL and TPL zones[23,30]. Saline lakes are usually tail-end waters and terrigenous refractory DOC accumulates along with water evaporation[12,31]. In contrast, glacial meltwater and rainwater commonly have low DOC concentrations (around 1.0 mg L^{-1} or lower)[32,33] and could dilute lake DOC in saline lakes. For lakes, Bositeng and Qinghai in the IMXL and TPL zones, decreased OC concentrations along with lake expansion have been reported[34,35].

https://doi.org/10.1038/s41467-024-52387-2

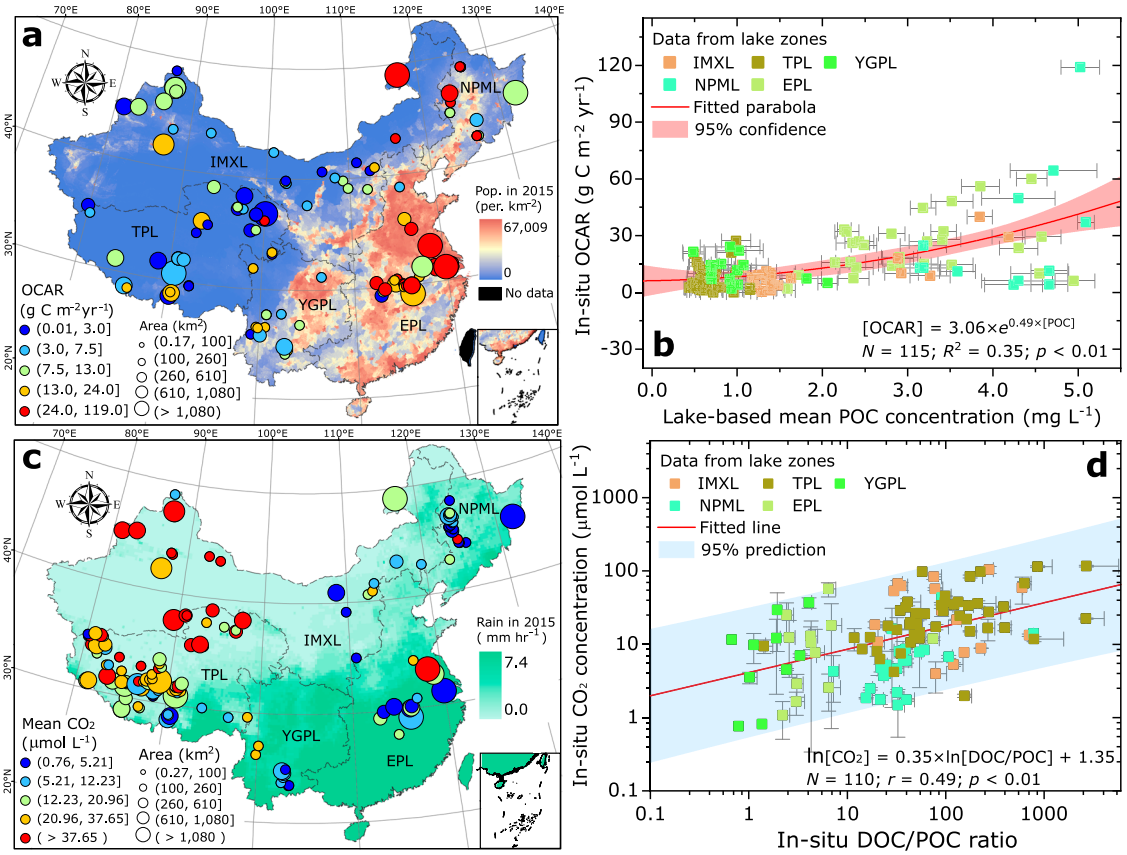

Fig. 4 | Implications of increasing DOC and POC concentrations. a OCAR data of 115 Chinese lakes and (**b**) their positive relation to POC concentrations. **c** Mean CO_2 concentrations of 149 lakes and (**d**) their positive correlation with DOC/POC ratios. Error bars indicate Standard deviation. OCAR: OC accumulation rate. Pop. in 2015: 1 km grid-based population density (person km^{-2}). Source data are provided as a Source Data file.

Strengthened wind mixing increased lake DOC concentrations in the southeast NPML, EPL, and YGPL zones during 1984–2023. For these three zones, wind speed increased for 58.0% of lakes (Supplementary Fig. 7g) and was the main factor influencing DOC changes in 70.6% of lakes (Fig. 3a). Wind disturbance likely increased lake DOC concentrations by promoting sediment DOC release, which was attributed to two favorable conditions. First, lakes in these zones are usually shallow with a mean water depth of 4.4 m[26] and are commonly characterized by strong sediment resuspension[36]. Second, high algal proliferation in these zones elevates the OC content of the sediment[19,37], which further leads to high DOC release from the pore water of sediment or from the photoproduction of OC in suspended sediment. For example, the suspended sediment of the eutrophic Lake Taihu had a DOC photoproduction of 0.29–0.83 mg L^{-1} [38].

For a specific lake, the changes of OC concentration had important effects on OC storage, especially for DOC storage. For the 1125 lakes with time-series data of water volume (Supplementary Figs. 8, 9), changes in DOC concentration accounted for an average of 68.2% of the annual variations in DOC storage. In comparison, changes in POC concentration explained an average of 38.4% of the annual variations in POC storage. Note that the effect of OC concentration on OC storage greatly differed across lakes.

Implications for carbon deposition and emission

As OC storage increased from 1984 to 2023, lakes played a positive role in contributing to China's goal of achieving carbon neutrality by 2060. Moreover, the amount of OC stored in lakes is expected to increase further. For the northwest TPL zone, lake water volume is expected to increase over the next 40 years[39]. For the southeast lakes, algal blooms are likely to increase due to climate warming[20]. In addition, the changes in OC concentration also have an essential influence on POC deposition to sediment and CO_2 emission to the atmosphere.

The burial of OC in lakes is an important method of carbon sequestration. Globally, lakes and reservoirs have a total OC burial rate of 150 Tg C yr^{-1}, which is positively correlated with water column-stored OC[4]. Across China, the OC accumulation rates (OCAR) of lakes with higher POC concentrations in the southeast were generally higher than those of lakes with lower POC concentrations in the northwest, with mean values of 22 ± 19.87 g C m^{-2} yr^{-1} and 7.78 ± 7.77 g C m^{-2} yr^{-1}, respectively (Figs. 1c, 4a). For different lakes, OCAR after the 1950s was exponentially related to the climatological mean POC concentration during 1984–2023, with $R^2 = 0.35$ and $p < 0.01$ (Fig. 4b). Based on the fitting formula and satellite-derived annual mean POC concentration, we estimated that total OC burial in Chinese lakes increased from 1.01 Tg C yr^{-1} in the 1980s to 1.13 Tg C yr^{-1} in the 2020s, with an increase of 11.0%. Therefore, increased lake POC concentration facilitated OC deposition to sediment during 1984–2023.

OC mineralization through microbial decomposition and photochemical oxidation acts as an essential CO_2 source[12,40]. Globally, lakes with high OC concentrations tend to also have high CO_2 emissions[5,41]. However, high POC concentrations also indicate high levels of photosynthesis, which consumes lake CO_2[1]. This study showed that in-situ CO_2 concentration was positively correlated with the ratio of DOC to POC (Fig. 4c, d). Consequently, we found that changes in both DOC and POC concentrations led to varying effects on lake CO_2 emissions from 1984 to 2023. For the southeast YGPL and EPL zones, 67.2% of lakes might have elevated CO_2 concentrations due to increased DOC (Fig. 1b). In contrast, for the northwest IMXL and TPL zones, 71.1% of lakes likely experienced a decrease in CO_2 concentration. This decline was primarily due to the reduction in DOC concentration caused by

lake expansion. Additionally, decreased water conductivity and increased nutrient input further enhanced CO_2 absorption through algal proliferation in these northwest zones[29].

Based on these findings, substantial changes may have also occurred in the global lake carbon cycle. Firstly, increases in lake OC storage are likely prevalent worldwide. Satellite monitoring globally indicated that 80% of lakes experienced surface area expansion during 2003–2018[21]. Moreover, increasing algal bloom frequency was detected in 62% of freshwater lakes during the 1980s–2010s[19]. Secondly, due to algal proliferation, elevated POC concentrations should increase POC deposition in sediments. For example, eutrophic lowland lakes in Europe exhibited OCAR values in excess of 50 g C m^{-2} yr^{-1} over the past century[42]. Thirdly, lake CO_2 emissions are expected to vary with water eutrophication and/or expansion. Eutrophication has been observed to decrease lake CO_2 emissions in the Midwestern U.S.[43] while expanded lakes in boreal western Canada have shifted from CO_2 sources to sinks[44]. These changes introduce significant uncertainties in estimating CO_2 emissions from global lakes using different datasets[5]. Therefore, urgent efforts are needed to monitor carbon storage in the water column, CO_2 emission to the atmosphere, and carbon burial in the sediment using global revisit satellite data.

Methods

Data acquisition

This study used in-situ data sampled during 2004–2023 (Dataset I in Supplementary Table 1, Supplementary Fig. 3). The in-situ data contain DOC, dissolved inorganic carbon (DIC), POC, Chl-a, TSM, pH, temperature, and conductivity values for 4,201 stations of 348 lakes. During field sampling, pH, temperature, and conductivity were recorded using a *YSI* Multi-parameter Sonde; lake water was filtrated through *Whatman* GF/F filters (0.7 μm pore size) to obtain DOC, DIC, POC, Chl-a, and TSM samples[45,46]. Then, in the lab, DOC, DIC, and POC concentrations were determined through the high-temperature combustion method[46]; TSM concentration was determined via gravimetry after drying; and Chl-a concentration was measured by the spectrophotometer technique[45].

This study also obtained publicly available data (Datasets II-X in Supplementary Table 1). Among them, daily surface reflectance of Landsat-5/7/8/9 satellites during 1984–2023 was accessed via the Google Earth Engine (GEE) platform; daily water storage during 1984–2023 was sourced from the GloLakes dataset[47]; lake polygon/area/depth and river network/basin in 2015 were obtained from the HydroSHEDS dataset[26]; moreover, from the European Centre for Medium-Range Weather Forecasts (ECMWF), we obtained monthly averaged basin property data during 1984–2023, including population density, digital elevation model (DEM), evaporation, leaf area index of high vegetation (LAI_HighVeg), leaf area index of low vegetation (LAI_LowVeg), runoff, air temperature at 2 m height (Temp2m), precipitation, and wind speed. In addition, we also acquired OCAR data after the 1950s for 115 lakes in China through meta-analysis.

Remote retrieval of DOC concentration and storage

Lake DOC concentration is related to basin properties[48], shows spatial variations within a single lake[17], and tends to be higher in saline lakes compared to freshwater ones[49]. Based on these insights, this study developed an algorithm to estimate DOC concentration from Landsat reflectance data. First, a multilayer back propagation neural network (MBPNN) with three hidden layers was trained to simulate lake-based annual mean DOC concentration using nine basin properties (Supplementary Fig. 4a). Second, using the simulated DOC, the matched Landsat reflectance at four visible and near-infrared bands (Supplementary Note 1), longitude, and latitude, two Random Forest models were built to retrieve DOC concentrations in freshwater and saline lakes, respectively, which were identified through a weighted decision tree method (Supplementary Note 2). The hyperparameters of the two Random Forests (Supplementary Note 2) were determined through the grid-search and K-fold cross-validation methods.

The parameterized models showed mean absolute percent difference (MAPD) values of 17.5% and 15.15% for the 30% testing data from freshwater and saline lakes, respectively (Supplementary Fig. 4b, c). The parameterized models were then applied to derive daily DOC concentrations from Landsat data, which had been processed to remove clouds and other non-water pixels using the pixel quality attributes provided by GEE. The developed models satisfactorily captured DOC concentrations from time-series Landsat data, with high values for saline/eutrophic lakes and low values for estuarine waters (Supplementary Fig. 10). Furthermore, annual mean DOC concentrations for 24,366 lakes during 1984–2023 were calculated using the satellite-derived daily DOC concentrations. Finally, DOC storage for 24,366 lakes in 2015 was calculated by multiplying annual mean DOC concentrations by water stocks from the HydroLAKES dataset[26]; annual DOC storage for 1125 lakes during 1984–2023 was calculated by multiplying annual mean DOC concentrations by water stocks from the GloLakes dataset[47].

Remote retrieval of POC concentration and storage

Several algorithms were proposed to remotely derive POC concentrations in inland/coastal waters, and Chinese lakes in the southwest Tibet Plateau usually have low POC concentrations[50,51]. Based on the existing progress, this study developed a two-step algorithm to retrieve POC concentration from Landsat reflectance data (Supplementary Fig. 5a). First, four empirical equations (Eq. (1)) were constructed to roughly estimate POC concentration using the DEM, longitude, red band reflectance (R_{red}), and normalized difference carbon index[51].

$$\begin{aligned}
&\ln(\mathrm{POC}) = -0.0005 \times [\mathrm{DEM}] + 1.13, R^2 = 0.39\\
&\ln(\mathrm{POC}) = 0.05 \times [\mathrm{Longitude}] - 4.18, R^2 = 0.42\\
&\ln(\mathrm{POC}) = 0.51 \times \ln(R_{red}) + 3.06, R^2 = 0.31\\
&\ln(\mathrm{POC}) = 1.72 \times [\mathrm{NDCI}] + 0.68, R^2 = 0.32\\
&[\mathrm{NDCI}] = (R_{red} + R_{blue})/(R_{red} - R_{blue})
\end{aligned} \tag{1}$$

where R_{blue} denotes the blue band reflectance. Second, a Random Forest model was trained to precisely retrieve POC concentration using the roughly estimated results (Eq. (1)), longitude, latitude, DEM, and the matched Landsat reflectance (Supplementary Note 1, Supplementary Table 2).

The parameterized model obtained MAPD values of 16.7% and 16.5% for the training and testing data, respectively (Supplementary Fig. 5b, c). When they were applied to time-series Landsat data, the developed models obtained reasonable POC concentrations, with high values for eutrophic/turbid lakes and estuarine waters (Supplementary Fig. 10). Then, similar to the DOC retrieval, the parameterized models were applied to obtain daily POC concentrations and annual mean POC concentrations for 24,366 lakes during 1984–2023, calculate POC storage for 24,366 lakes in 2015, and calculate annual POC storage for 1125 lakes during 1984–2023.

Lake CO_2 concentration calculation

Using the in-situ pH, temperature, and DIC data (Dataset I in Supplementary Table 1), this study calculated CO_2 concentration based on the carbonate equilibrium method[52]. The method is commonly adopted when there is no in-situ CO_2[53]. The method is shown as Eq. (2):

$$\begin{aligned}
[\mathrm{CO_2}] &= [\mathrm{DIC}] / \left(\frac{K_1}{[\mathrm{H^+}]} + \frac{K_1 \times K_2}{[\mathrm{H^+}]^2} + 1 \right)\\
[\mathrm{H^+}] &= 10^{-\mathrm{pH}}
\end{aligned} \tag{2}$$

where $[CO_2]$ is the CO_2 concentration (μmol L^{-1}); $[H^+]$ indicates the H^+ concentration (mol L^{-1}); [DIC] denotes the DIC concentration (μmol L^{-1}); K_1 and K_2 are the ionization fractions, which are calculated using water temperature (T_w) via Eq. (3).

$$\log_{10}K_1 = a_1 + b_1T_w + c_1/T_w + d_1\log_{10}T_w + e_1/(T_w)^2$$
$$\log_{10}K_2 = a_2 + b_2T_w + c_2/T_w + d_2\log_{10}T_w + e_2/(T_w)^2 \quad (3)$$

where a_1, a_2, b_1, b_2, c_1, c_2, d_1, d_2, e_1, and e_2 are constants[52].

Statistical analyses

This study matched Landsat reflectance for the measured DOC and POC concentrations (Supplementary Note 1), developed a weighted decision tree method to identify freshwater and saline lake types (Supplementary Note 2), delineated lake basin boundaries for 24,366 lakes (Supplementary Note 3), and calculated relative contributions of different factors to variations in DOC and POC concentrations through the nonlinear Random Forest analyses (Supplementary Note 4). Moreover, we did regression analyses to determine the relationships between two variables and the changing trend of one variable along with time, with a significance level $p < 0.05$ (two-tailed test) being significant.

Data availability

All the used time-series Landsat-5/7/8/9 reflectance datasets are available at https://developers.google.com/earth-engine/datasets/catalog/landsat. The GloLakes dataset of lake water volume is available at https://doi.org/10.25914/K8ZF-6G46. The HydroLAKES, HydroRIVERS, and HydroBASINS datasets used in this study are available at https://www.hydrosheds.org/products. The population density data are available at https://www.resdc.cn/DOI/DOI.aspx?DOIID=32. The DEM data are available at https://lpdaac.usgs.gov/products/srtmgl1v003/. The lake basin property data are available at https://cds.climate.copernicus.eu/cdsapp#!/dataset/reanalysis-era5-land-monthly-means?tab=overview. The DOC and POC data generated in this study have been deposited in the Figshare repository under accession code https://doi.org/10.6084/m9.figshare.26488966[54]. Source data are provided with this paper.

Code availability

Source codes for POC retrieval from Landsat data are available at https://code.earthengine.google.com/fb14d077d79b91cf116d17cade3f5730. Source codes for DOC retrieval from Landsat data are available at https://code.earthengine.google.com/a1eedef98d1f1a0780fe6afd97b34efb and from Zenodo at https://doi.org/10.5281/zenodo.13234019[55]. Other source codes used in this study are also publicly available from Zenodo at https://doi.org/10.5281/zenodo.13234019[55].

References

1. Tranvik, L. J. et al. Lakes and reservoirs as regulators of carbon cycling and climate. *Limnol. Oceanogr.* **54**, 2298–2314 (2009).
2. Regnier, P., Resplandy, L., Najjar, R. G. & Ciais, P. The land-to-ocean loops of the global carbon cycle. *Nature* **603**, 401–410 (2022).
3. Drake, T. W., Raymond, P. A. & Spencer, R. G. M. Terrestrial carbon inputs to inland waters: a current synthesis of estimates and uncertainty. *Limnol. Oceanogr. Lett.* **3**, 132–142 (2017).
4. Mendonça, R. et al. Organic carbon burial in global lakes and reservoirs. *Nat. Commun.* **8**, 1694 (2017).
5. Raymond, P. A. et al. Global carbon dioxide emissions from inland waters. *Nature* **503**, 355–359 (2013).
6. Bauer, J. E. et al. The changing carbon cycle of the coastal ocean. *Nature* **504**, 61–70 (2013).
7. Artifon, V., Zanardi-Lamardo, E. & Fillmann, G. Aquatic organic matter: classification and interaction with organic microcontaminants. *Sci. Total Environ.* **649**, 1620–1635 (2019).
8. Song, K. et al. Quantification of dissolved organic carbon (DOC) storage in lakes and reservoirs of mainland China. *J. Environ. Manag.* **217**, 391–402 (2018).
9. Zhang, Y., van Dijk, M. A., Liu, M., Zhu, G. & Qin, B. The contribution of phytoplankton degradation to chromophoric dissolved organic matter (CDOM) in eutrophic shallow lakes: Field and experimental evidence. *Water Res.* **43**, 4685–4697 (2009).
10. Ministry of Ecology and Environment, China (MEEC). Environmental quality standards for surface water (GB 3838-2002). Beijing (2002).
11. Aizaki, M., Otsuki, A., Fukushima, T., Hosomi, M. & Muraoka, K. Application of Carlson's trophic state index to Japanese lakes and relationships between the index and other parameters. *Int. Ver. für. Theoretische und Angew. Limnologie Verhandlungen* **21**, 675–681 (1981).
12. Bianchi, T. S. The role of terrestrially derived organic carbon in the coastal ocean: a changing paradigm and the priming effect. *Proc. Natl Acad. Sci. USA* **108**, 19473–19481 (2011).
13. Baines, S. B. & Pace, M. L. The production of dissolved organic matter by phytoplankton and its importance to bacteria: Patterns across marine and freshwater systems. *Limnol. Oceanogr.* **36**, 1078–1090 (1991).
14. Liu, D., Du, Y., Yu, S., Luo, J. & Duan, H. Human activities determine quantity and composition of dissolved organic matter in lakes along the Yangtze River. *Water Res.* **168**, 115132 (2020).
15. Butturini, A. et al. Origin, accumulation and fate of dissolved organic matter in an extreme hypersaline shallow lake. *Water Res.* **221**, 118727 (2022).
16. Liu, D. et al. Three-dimensional observations of particulate organic carbon in shallow eutrophic lakes from space. *Water Res.* **229**, 119519 (2023).
17. Liu, D., Yu, S., Xiao, Q., Qi, T. & Duan, H. Satellite estimation of dissolved organic carbon in eutrophic Lake Taihu, China. *Remote Sens. Environ.* **264**, 112572 (2021).
18. Jenny, J.-P. et al. Scientists' warning to humanity: rapid degradation of the world's large lakes. *J. Gt. Lakes Res.* **46**, 686–702 (2020).
19. Hou, X. et al. Global mapping reveals increase in lacustrine algal blooms over the past decade. *Nat. Geosci.* **15**, 130–134 (2022).
20. Ho, J. C., Michalak, A. M. & Pahlevan, N. Widespread global increase in intense lake phytoplankton blooms since the 1980s. *Nature* **574**, 667–670 (2019).
21. Luo, S. et al. Satellite laser altimetry reveals a net water mass gain in global lakes with spatial heterogeneity in the early 21st century. *Geophys. Res. Lett.* **49**, e2021GL096676 (2022).
22. Yao, T. et al. Multispherical interactions and their effects on the Tibetan Plateau's earth system: a review of the recent researches. *Natl Sci. Rev.* **2**, 468–488 (2015).
23. Zhang, G. et al. Regional differences of lake evolution across China during 1960s–2015 and its natural and anthropogenic causes. *Remote Sens. Environ.* **221**, 386–404 (2019).
24. Huang, C. et al. Long-term variation of phytoplankton biomass and physiology in Taihu Lake as observed via MODIS satellite. *Water Res.* **153**, 187–199 (2019).
25. Nanjing Institute of Geography and Limnology Chinese Academy of Sciences (NIGLAS). National lake survey report. (Science Press, 2019).
26. Messager, M. L., Lehner, B., Grill, G., Nedeva, I. & Schmitt, O. Estimating the volume and age of water stored in global lakes using a geo-statistical approach. *Nat. Commun.* **7**, 13603 (2016).
27. Tong, Y. et al. Decline in Chinese lake phosphorus concentration accompanied by shift in sources since 2006. *Nat. Geosci.* **10**, 507–511 (2017).
28. Jiang, G. et al. An absorption-specific approach to examining dynamics of particulate organic carbon from VIIRS observations in inland and coastal waters. *Remote Sens. Environ.* **224**, 29–43 (2019).

29. Pi, X. et al. Chlorophyll-a concentrations in 82 large alpine lakes on the Tibetan Plateau during 2003–2017: temporal-spatial variations and influencing factors. *Int. J. Digit. Earth* **14**, 714–735 (2021).
30. Song, C. et al. Widespread declines in water salinity of the endorheic Tibetan Plateau lakes. *Environ. Res. Commun.* **4**, 091002 (2022).
31. Song, K. et al. Characterization of CDOM in saline and freshwater lakes across China using spectroscopic analysis. *Water Res.* **150**, 403–417 (2019).
32. Gao, T. et al. Characterization, sources and transport of dissolved organic carbon and nitrogen from a glacier in the Central Asia. *Sci. Total Environ.* **725**, 138346 (2020).
33. Safieddine, S. A. & Heald, C. L. A global assessment of dissolved organic carbon in Precipitation. *Geophys. Res. Lett.* **44**, 11,672–11,681 (2017).
34. Li, Z. et al. Temporal and spatial distribution and fluorescence spectra of dissolved organic matter in plateau lakes: a case study of Qinghai Lake. *Water* **13**, 3481 (2021).
35. Narengerile & Wang, H.-J. The spatial and temporal characteristics of water quality in Bosten Lake. *Guangdong Agric. Sci.* **44**, 99–103 (2017).
36. Liu, D. et al. Observations of water transparency in China's lakes from space. *Int. J. Appl. Earth Obs.* **92**, 102187 (2020).
37. Wang, M. et al. Carbon accumulation and sequestration of lakes in China during the Holocene. *Glob. Change Biol.* **21**, 4436–4448 (2015).
38. Hu, B., Wang, P., Zhang, N., Wang, C. & Ao, Y. Photoproduction of dissolved organic carbon and inorganic nutrients from resuspended lake sediments. *Environ. Sci. Pollut. Res. Int.* **23**, 22126–22135 (2016).
39. Xu, F. et al. Widespread societal and ecological impacts from projected Tibetan Plateau lake expansion. *Nat. Geosci.* **17**, 516–523 (2024).
40. Lapierre, J. F., Guillemette, F., Berggren, M. & del Giorgio, P. A. Increases in terrestrially derived carbon stimulate organic carbon processing and CO_2 emissions in boreal aquatic ecosystems. *Nat. Commun.* **4**, 2972 (2013).
41. Wen, Z. et al. Carbon dioxide emissions from lakes and reservoirs of China: a regional estimate based on the calculated pCO_2. *Atmos. Environ.* **170**, 71–81 (2017).
42. Anderson, N. J., Bennion, H. & Lotter, A. F. Lake eutrophication and its implications for organic carbon sequestration in Europe. *Glob. Change Biol.* **20**, 2741–2751 (2014).
43. Pacheco, F., Roland, F. & Downing, J. Eutrophication reverses whole-lake carbon budgets. *Inland Waters* **4**, 41–48 (2014).
44. Kuhn, M. A. et al. Opposing effects of climate and permafrost thaw on CH_4 and CO_2 emissions from northern lakes. *AGU Adv.* **2**, e2021AV000515 (2021).
45. Mueller, J. L. et al. Ocean optics protocols for satellite ocean color sensor validation, Revision 4, Volume III: Radiometric Measurements and Data Analysis Protocols, NASA/TM-2003-211621/Rev4-Vol. III, p. 78 (NASA Goddard Space Flight Center, Greenbelt, Maryland, 2003).
46. Knap, A. H., Michaels, A. F., Close, A. R., Ducklow, H. W. & Dickson, A. G. Protocols for the joint global ocean flux study (JGOFS) core measurements. 119–142 (JGOFS, 1996).
47. Hou, J., Van Dijk, A. I. J. M., Renzullo, L. J. & Larraondo, P. R. GloLakes: water storage dynamics for 27 000 lakes globally from 1984 to present derived from satellite altimetry and optical imaging. *Earth Syst. Sci. Data* **16**, 201–218 (2024).
48. Toming, K. et al. Predicting lake dissolved organic carbon at a global scale. *Sci. Rep.* **10**, 8471 (2020).
49. Song, K. et al. Dissolved carbon in a large variety of lakes across five limnetic regions in China. *J. Hydrol.* **563**, 143–154 (2018).
50. Liu, D. et al. Mapping particulate organic carbon in lakes across China using OLCI/Sentinel-3 imagery. *Water Res.* **250**, 121034 (2024).
51. Son, Y. B., Gardner, W. D., Mishonov, A. V. & Richardson, M. J. Multispectral remote-sensing algorithms for particulate organic carbon (POC): The Gulf of Mexico. *Remote Sens. Environ.* **113**, 50–61 (2009).
52. Stumm, W. & Morgan, J. J. *Aquatic chemistry: chemical equilibria and rates in natural waters*. (Wiley-Interscience, 1996).
53. Weyhenmeyer, G. A. et al. Significant fraction of CO_2 emissions from boreal lakes derived from hydrologic inorganic carbon inputs. *Nat. Geosci.* **8**, 933–936 (2015).
54. Liu, D. The satellite-derived datasets of organic carbon concentration and storage in 24,366 Chinese lakes. Figshare, https://doi.org/10.6084/m9.figshare.26488966.v1 (2024).
55. Liu, D. Source code for remotely retrieving organic carbon concentrations and storage in lakes. Zenodo, https://doi.org/10.5281/zenodo.13234019 (2024).

Acknowledgements

We acknowledge the National Aeronautics and Space Administration, Google Earth Engine, and the European Centre for Medium-Range Weather Forecasts for providing Landsat reflectance and/or basin property data. This study was supported by the National Natural Science Foundation of China (Grants U22A20561, 42271376, 41930760 and 42425104) to K.S., D.L., Y.Z. and H.D., the Youth Innovation Promotion Association CAS (Grant #2021313) to D.L., the Second Tibetan Plateau Scientific Expedition and Research Program (STEP) (Grant 2019QZKK0202) to K.S., the NIGLAS Foundation (Grant #E1SL002) to K.S. R.I.W. was supported by a UKRI Natural Environment Research Council (NERC) Independent Research Fellowship [NE/T011246/1] and a NERC grant reference number NE/X019071/1, UK EO Climate Information Service.

Author contributions

D.L. proposed the concepts and wrote the original manuscript. K.S. and H.D. proposed the concepts, supervised the project, and helped with manuscript editing. N.Y. helped with data processing and validation. P.C., L.R., T.K., A.T., E.S., R.W., and Y.Z. helped edit the manuscript.

Competing interests

The authors declare no competing interests.

Ethics approval

We support inclusive, diverse, and equitable conduct of research. We have followed ethical guidelines and obtained all necessary approvals for our work.

Additional information

Supplementary information The online version contains supplementary material available at https://doi.org/10.1038/s41467-024-52387-2.

Correspondence and requests for materials should be addressed to Kun Shi or Hongtao Duan.

Peer review information *Nature Communications* thanks the anonymous reviewers for their contribution to the peer review of this work. A peer review file is available.